

OPTIMAL DESIGN OF SPACECRAFT FORMATIONS IN LISSAJOUS ORBITS

Sergey Shestakov^{*}, Sergey Trofimov[†], and Maksim Shirobokov[‡]

A semianalytical optimisation technique is developed for the design of Lissajous orbit formations near a collinear libration point. It is based on the use of Lindstedt-Poincaré series that approximate the center manifold. Any performance factor can be constructed by symbolically manipulating the series. In this study, we consider two relative distance-based scalar metrics intended for a general/projected circular orbit formation. In the first-order approximation, the relative motion parameters can be optimised analytically or by a simple numerical routine. These values are then exploited as an initial guess in the numerical optimisation procedure for the 15th-order approximation model. The Nelder-Mead simplex method implemented in MATLAB's `fminsearch` function is used. Finally, all the trajectories are adapted to the ephemeris model, which requires 3-8 multiple-shooting iterations.

INTRODUCTION

In contrast to the case of near-Earth formations, the design of a libration point formation is a much more difficult and less studied procedure. The primary obstacle is the unstable and highly nonlinear dynamics in the vicinity of the collinear libration points. The first works dated back at the beginning of the 2000s aimed at designing a continuous or impulsive control law that ensures keeping the predefined formation geometry.^{1-3,5,6} The idea of concurrent numerical optimisation of both formation configuration and control parameters has also been suggested.⁷ At the same time, the general trend of maximally exploiting the natural dynamics was then observed, starting with the study of Howell and Marchand who introduced the concept of the natural formation, a formation that keeps favourable geometry under no control (i.e., in purely ballistic motion).⁸ The efforts to explicitly describe and visualise the set of best (slowest-degrading) initial configurations for a two-spacecraft formation resulted in the notions of zero relative radial acceleration and zero relative acceleration and velocity regions.^{9,10} All the criteria based on the relative acceleration are, however, indirect and approximate: the two spacecraft are assumed to move in close orbits with synchronised velocities. Moreover, the above notions become useless for the design of non-rigid formations with relative distances changing in a prescribed way. Even the problem of rigid formation design with three or more spacecraft is tractable only numerically. For example, in the recent work of Ferrari and Lavagna, the genetic algorithm is utilised for global optimisation.¹¹

^{*}Corresponding author, Ph.D. Candidate, Junior Researcher, Space Systems Dynamics Department, Keldysh Institute of Applied Mathematics, 4 Miusskaya Sq., 125047 Moscow, Russia; shestakov.sa@gmail.com

[†]Ph.D., Researcher, Space Systems Dynamics Department, Keldysh Institute of Applied Mathematics, 4 Miusskaya Sq., 125047 Moscow, Russia

[‡]Ph.D., Researcher, Space Systems Dynamics Department, Keldysh Institute of Applied Mathematics, 4 Miusskaya Sq., 125047 Moscow, Russia

CENTRAL MANIFOLD DYNAMICS IN THE VICINITY OF COLLINEAR LIBRATION POINTS

In the current research, a novel semianalytical technique is proposed for the Lissajous orbit formation design. Its foundation is the use of Lindstedt-Poincaré (LP) series that approximate the center manifold in the vicinity of the libration point. The LP expansion explicitly parameterises—up to the user-specified degree of accuracy—the invariant tori the manifold is foliated by. The equations of spacecraft motion have the following nondimensional form

$$\begin{aligned}\ddot{X} - 2\dot{Y} &= U_X \\ \ddot{Y} + 2\dot{X} &= U_Y \\ \ddot{Z} &= U_Z\end{aligned}\tag{1}$$

where

$$U(X, Y, Z) = \frac{X^2 + Y^2}{2} + \frac{1 - \mu}{R_1} + \frac{\mu}{R_2}$$

is the effective potential, U_X , U_Y and U_Z are the partial derivatives of U with respect to the position variables, and $\mu = m_2/(m_1 + m_2)$ is the mass parameter of the system. The distances to the celestial bodies are given by the equalities

$$\begin{aligned}R_1 &= \sqrt{(X + \mu)^2 + Y^2 + Z^2} \\ R_2 &= \sqrt{(X - 1 + \mu)^2 + Y^2 + Z^2}\end{aligned}$$

The system (1) has five equilibrium points called libration or Lagrangian points. Three of them lying on the X -axis, are named collinear. Usually denoted by L_1 , L_2 , and L_3 , these points are proved to be unstable. In the Sun-Earth system, the coordinates of the L_1 and L_2 points are as follows:

$$X_{L1} = 0.9899871, \quad X_{L2} = 1.0100740$$

Linearisation About the Collinear Libration Point

The LP series are usually written in the libration point-centered frame with the dimensionless coordinates $x = (X - X_L)/D$, $y = Y/D$, $z = Z/D$ where X , Y , and Z are the coordinates in the synodic frame with an origin at the barycenter of two massive celestial bodies, X_L is the x -coordinate of the libration point in hand (L_1 or L_2), and $D = |X_L - 1 + \mu|$ is the distance from this libration point to the smaller body. Then, the evolution of the position vector $\mathbf{r} = (x, y, z)^T$ is described in the linear approximation by the equations

$$\begin{aligned}x &= \alpha \cos(\omega_p t + \phi_1) \\ y &= -\kappa \alpha \sin(\omega_p t + \phi_1) \\ z &= \beta \cos(\omega_v t + \phi_2)\end{aligned}\tag{2}$$

The constants α and β play a role of the planar and vertical amplitudes, respectively; ϕ_1 and ϕ_2 are the arbitrary phases, and

$$\kappa = \frac{\omega_p^2 + 2\omega_v^2 + 1}{2\omega_p}\tag{3}$$

Lindstedt-Poincaré Series

The LP series expansion explicitly parameterizes—up to the user-specified degree of accuracy—the invariant tori the center manifold is foliated by. In particular, the manifolds consisting of periodic and quasi-periodic libration point orbits can be approximated by the LP series.

The general expressions of order n for the Lissajous orbits have the following complex exponential form:¹²

$$\begin{aligned} x &= \sum x_{ijkm} \alpha^i \beta^j \gamma_1^k \gamma_2^m \\ y &= \sqrt{-1} \sum y_{ijkm} \alpha^i \beta^j \gamma_1^k \gamma_2^m \\ z &= \sum z_{ijkm} \alpha^i \beta^j \gamma_1^k \gamma_2^m \end{aligned} \quad (4)$$

Here $\gamma_i = \exp[\sqrt{-1}(\omega_i t + \phi_i)]$, and the summation is performed over the indices satisfying the conditions $I = \{i, j \geq 0, |k| \leq i, |m| \leq j, 1 \leq i + j \leq n\}$. The frequencies ω_1 and ω_2 are also expanded:

$$\begin{aligned} \omega_1 &= \omega_p + \sum d_{ij} \alpha^i \beta^j \\ \omega_2 &= \omega_v + \sum f_{ij} \alpha^i \beta^j \end{aligned} \quad (5)$$

The indices in Eq. (5) are summed over the positive even numbers. In the Sun-Earth system, the planar and vertical frequencies ω_p and ω_v are respectively equal to 2.0864519 and 2.0152089 for the L_1 point; for the L_2 point, their values are 2.0570158 and 1.9850765.

The LP series for halo orbits, three-dimensional periodic orbits branching from the family of planar orbits, can be found in.¹³ The expressions resemble Eq. (4), except for the fact that a single frequency $\omega = \omega_1 = \omega_2$ appears and the additional condition for such a resonance is required to be satisfied. We further concentrate on the family of Lissajous orbits, though the methodology proposed can also be applied to halo orbit formations and corresponding LP series.

ANALYTICAL ESTIMATES BASED ON THE LINEAR APPROXIMATION

The reference orbit approximated by the LP series expansion of any order is described by four parameters: two amplitudes α, β and two phases ϕ_1, ϕ_2 . Assuming the first spacecraft in a two-spacecraft formation moves along the reference orbit, the relative position vector

$$\Delta \mathbf{r} = \mathbf{r}_2 - \mathbf{r}_1 = \begin{bmatrix} x_2 - x_1 \\ y_2 - y_1 \\ z_2 - z_1 \end{bmatrix} \equiv \begin{bmatrix} \Delta x \\ \Delta y \\ \Delta z \end{bmatrix}$$

can be readily expanded in LP series by subtracting the series for the components of \mathbf{r}_2 and \mathbf{r}_1 . The resulting LP expansions for $\Delta x, \Delta y$, and Δz can be parameterised by two differential amplitudes $\Delta\alpha, \Delta\beta$ and two differential phases $\Delta\phi_1, \Delta\phi_2$.

To measure the performance of a formation, some performance metric should be introduced. If the relative distance is of primary interest in the mission, it is convenient to choose such a metric to be

$$\Delta_1 = \Delta r^2 = \Delta x^2 + \Delta y^2 + \Delta z^2$$

When a projection of the relative trajectory onto the plane with the unit normal vector $\mathbf{n} = (n_x, n_y, n_z)^T$ is tracked, the following metric can be used:

$$\Delta_2 = \Delta r^2 - (\Delta \mathbf{r} \cdot \mathbf{n})^2 = (1 - n_x^2) \Delta x^2 + (1 - n_y^2) \Delta y^2 + (1 - n_z^2) \Delta z^2 - 2n_x n_y \Delta x \Delta y - 2n_y n_z \Delta y \Delta z - 2n_x n_z \Delta x \Delta z$$

If the projection plane is fixed in the rotating reference frame, \mathbf{n} is a constant vector.

The critical advantage of the proposed approach is the ability to compute the performance metric without the necessity of numerical integration in the highly unstable dynamical environment. It is also better to avoid the derivative computations due to the highly irregular search space. Along with the relatively small number of optimised variables, this all speaks in favour of derivative-free numerical optimisation techniques.

It is important to properly initialise the optimisation algorithm. The role of an initial guess grows with the increase of computational complexity of the problem (for instance, when the number of optimised variables is large). It appears that a good initial guess and performance metric estimates in the problem of libration point formation design can be obtained from the linear approximation.

In a two-spacecraft formation, the relative position vector $\Delta \mathbf{r}$ satisfies the same linearised equations of motion as do the position vectors of both spacecraft. Thus, the solution can be written in the same form as Eq. (2):

$$\begin{aligned} \Delta x &= A_x \cos(\omega_p t + \theta_1) \\ \Delta y &= -\kappa A_x \sin(\omega_p t + \theta_1) \\ \Delta z &= A_z \cos(\omega_v t + \theta_2) \end{aligned}$$

The transformation formulas between the relative amplitudes and phases $A_x, A_z, \theta_1, \theta_2$ and the above mentioned differential parameters $\Delta\alpha, \Delta\beta, \Delta\phi_1, \Delta\phi_2$ are presented in Appendix.

Distance metric

In the linear approximation, the squared relative distance is expressed as

$$\Delta_1 = \frac{A_x^2 (\kappa^2 + 1) + A_z^2}{2} + \frac{A_z^2}{2} \cos(2\omega_v t + 2\theta_2) - \frac{A_x^2 (\kappa^2 - 1)}{2} \cos(2\omega_p t + 2\theta_1)$$

It exhibits beating around the mean value

$$c^2 = \frac{A_x^2 (\kappa^2 + 1) + A_z^2}{2}$$

with the beat frequency $\delta = \omega_p - \omega_v$.

It follows from the beating theory that the upper and lower envelopes for the sum of two harmonics

$$a \cos(\omega t + \varphi) + b \cos((\omega + \Delta\omega)t + \varphi + \Delta\varphi)$$

are determined by the functions

$$\pm \sqrt{a^2 + b^2 + 2ab \cos(\Delta\omega \cdot t + \Delta\varphi)}$$

In our notation,

$$a = \frac{A_z^2}{2}, \quad b = -\frac{A_x^2(\kappa^2 - 1)}{2}, \quad \Delta\omega = 2\delta, \quad \Delta\varphi = -2\Delta\theta$$

where $\Delta\theta = \theta_2 - \theta_1$. So, the upper envelope has a form of

$$\sqrt{\frac{A_x^4(\kappa^2 - 1)^2}{4} + \frac{A_z^4}{4} - \frac{A_x^2 A_z^2(\kappa^2 - 1)}{2} \cos(2\delta t - 2\Delta\theta)} \quad (6)$$

For long time intervals, the extrema of the upper and lower envelopes representing the maximum and minimum values of Δr^2 significantly deviate from the mean value c^2 . Indeed, the relative deviation

$$\frac{\max |\Delta r^2 - c^2|}{c^2} = \frac{A_z^2 + A_x^2(\kappa^2 - 1)}{A_z^2 + A_x^2(\kappa^2 + 1)}$$

has a minimum of

$$\chi = \frac{\kappa^2 - 1}{\kappa^2 + 1} \approx 0.82$$

when $A_z = 0$. The distance between the spacecraft oscillates from $\sqrt{0.18 c^2} \approx 0.42 c$ to $\sqrt{1.82 c^2} \approx 1.35 c$ in this case (see Figure 1). Such variations would almost always be unacceptable in a real mission. However, it is important for us to observe that, if the harmonics interfere destructively, a time interval exists during which the squared relative distance values are confined within a strip of arbitrarily small width 2ε centered at c^2 . The larger the width, the longer this interval.

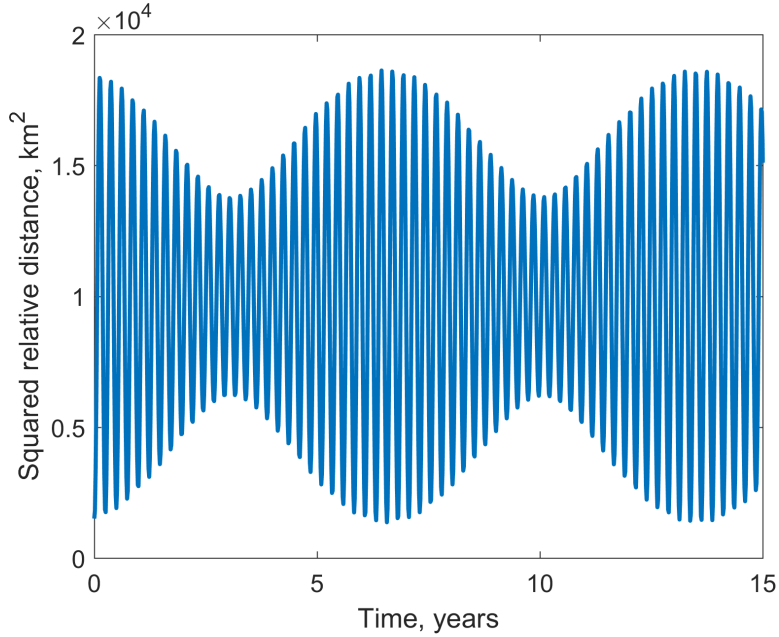


Figure 1. Distance metric behaviour without optimisation

To maximise its length for a given ε , we need to select the amplitudes A_x and A_z so that the distance between the adjacent roots of the equation

$$\sqrt{\frac{A_x^4(\kappa^2 - 1)^2}{4} + \frac{A_z^4}{4} - \frac{A_x^2 A_z^2(\kappa^2 - 1)}{2} \cos(2\delta t - 2\Delta\theta)} = c^2 \varepsilon$$

with respect to t is maximum. Returning to the short notation in terms of a and b , this equation can be rearranged as

$$\cos(2\delta t - 2\Delta\theta) = \frac{c^4\varepsilon^2 - a^2 - b^2}{2ab}$$

Taking into account the mean value constraint

$$a - b/\chi = c^2$$

yields

$$\cos(2\delta t - 2\Delta\theta) = \frac{c^4\varepsilon^2 - a^2 - \chi^2(a - c^2)^2}{2\chi a(a - c^2)}$$

The maximum distance between the roots is attained when the right-hand side is minimum. Dividing both the numerator and the denominator by c^4 and introducing the notation

$$\xi = 1 - \frac{a}{c^2}, \quad \xi \in [0, 1]$$

we obtain the equivalent function to be minimised:

$$\eta(\xi) = \frac{(1 - \xi)^2 + \chi^2\xi^2 - \varepsilon^2}{2\chi\xi(1 - \xi)}$$

This point

$$\xi_{\min} = \frac{1 - \varepsilon^2 - \sqrt{(1 - \varepsilon^2)(\chi^2 - \varepsilon^2)}}{1 - \chi^2}$$

does not depend on ε and can therefore be estimated with the assumption $\varepsilon = 0$:

$$\xi_{\min} \approx \frac{1}{1 + \chi} \approx 0.55$$

It results in the relationship

$$a = -b = \frac{\kappa^2 - 1}{2\kappa^2} c^2$$

or, in terms of the amplitudes,

$$A_x = \frac{c}{\kappa}, \quad A_z = \frac{c}{\kappa} \sqrt{\kappa^2 - 1} \quad (7)$$

The upper envelope curve is now determined by the function

$$\frac{c^2}{\kappa^2} (\kappa^2 - 1) |\sin(\delta t - \Delta\theta)|$$

To start with a favourable destructive interference interval, it is required to tune the relative phase difference $\Delta\theta$. Up to an integer multiple of π ,

$$|\Delta\theta| = \arcsin\left(\frac{\varepsilon\kappa^2}{\kappa^2 - 1}\right) \quad (8)$$

Then, the squared distance remains close enough (i.e., within the 2ε -strip) to the mean value over the interval $[0, T]$ where

$$T = \frac{2|\Delta\theta|}{\delta} \quad (9)$$

The formulas (7-9) can be exploited as an initial guess in a numerical optimisation procedure in case we aim at designing a two-spacecraft formation with the target relative distance c (see Figure 2).

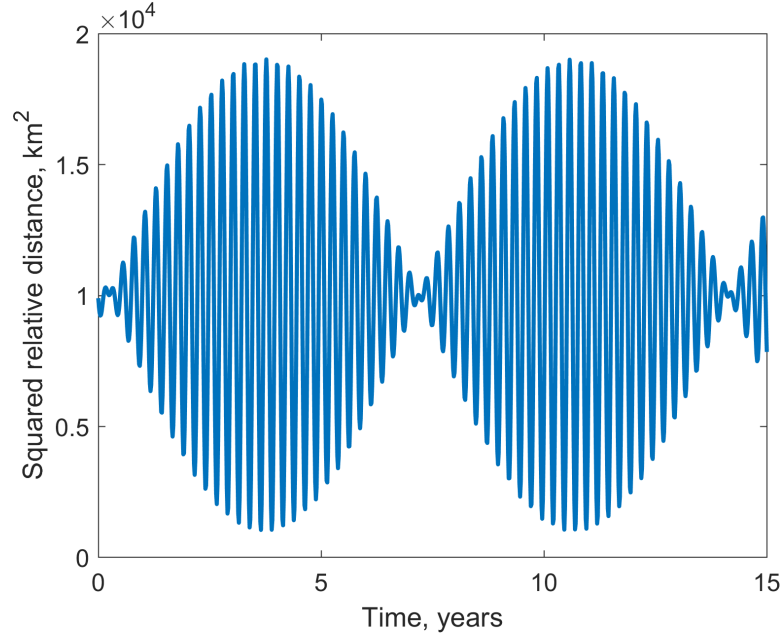


Figure 2. Optimised distance metric behaviour

Projected relative metric

Direct calculations show that

$$\Delta_2 = \frac{C}{2} + A \cos(\delta t + \Delta\theta) + B \sin(\delta t + \Delta\theta) + F_1(t) \cos(2\omega_p t + 2\theta_1) + F_2(t) \sin(2\omega_p t + 2\theta_1),$$

where $\delta = \omega_p - \omega_v$ is the slow frequency, C is the constant term,

$$C = A_x^2 (1 + \kappa^2 - n_x^2 - \kappa^2 n_y^2) + A_z^2 (1 - n_z^2),$$

A and B are amplitudes for slow oscillations $A = -A_x A_z n_x n_z$, $B = -A_x A_z \kappa n_y n_z$. The remaining motion is fast oscillations with frequency ω_p , whereas amplitudes are equal to

$$F_1(t) = \frac{A_x^2}{2} (1 - \kappa^2 - n_x^2 + \kappa^2 n_y^2) - A_x A_z n_x n_z \cos(\delta t + \Delta\theta) + A_x A_z \kappa n_y n_z \sin(\delta t + \Delta\theta) \\ + \frac{A_z^2}{2} (1 - n_z^2) \cos(2\delta t + 2\Delta\theta)$$

$$F_2(t) = A_x^2 \kappa n_x n_y + A_x A_z n_x n_z \sin(\delta t + \Delta\theta) + A_x A_z \kappa n_y n_z \cos(\delta t + \Delta\theta) \\ - \frac{A_z^2}{2} (1 - n_z^2) \sin(2\delta t + 2\Delta\theta)$$

For obtaining upper and lower envelopes of Δ_2 we define $q = \delta t + \Delta\theta$ to be the slow motion. Then,

$$F_1^2 + F_2^2 = A_0 + A_1 \cos q + B_1 \sin q + A_2 \cos 2q + B_2 \sin 2q.$$

The expressions for the coefficients A_i and B_i are presented in the Appendix. Then two envelopes are determined by the functions

$$E_{\pm} = \frac{C}{2} + A \cos q + B \sin q \pm \sqrt{A_0 + A_1 \cos q + B_1 \sin q + A_2 \cos 2q + B_2 \sin 2q}$$

As in the case of distance metric for a given small ε we want to maximise the length of such an interval that Δ_2 in it is bounded by $\varepsilon \cdot c_{mean}$, so again ε determines the width of strip. To achieve a desired result we maximise the difference between upper and lower envelopes $E_+ - E_-$.

To maximise the difference we solve the equation

$$2\sqrt{A_0 + A_1 \cos q + A_2 \cos 2q + B_1 \sin q + B_2 \sin 2q} - \varepsilon \cdot c_{mean} = 0$$

and we maximise the distance between such two adjacent roots that the left-hand side of the equation is negative on whole interval. Here ε is a small parameter, but c_{mean} could deviate from actual integral mean of the metric, rather it is the desired mean value of the metric oscillations. The accurate numerical optimisation does not produce a robust result when applied directly to a given problem. To achieve a better outcome we solve the equation of the type

$$c_0 + c_1 \cos q + s_1 \sin q + c_2 \cos 2q + s_2 \sin 2q = 0$$

using tangent half-angle substitution $\sin q = \frac{2u}{1+u^2}$, $\cos q = \frac{1-u^2}{1+u^2}$. The resulting polynomial equation

$$(c_0 + c_1 + c_2) + (2s_1 + 4s_2)u + (2c_0 - 6c_2)u^2 + (2s_1 - 4s_2)u^3 + (c_0 - c_1 + c_2)u^4 = 0$$

could be solved numerically. The roots of the original equation are given by $q = 2 \arctan t$. On the each interval between the roots the sign of the polynomial as well as the original trigonometric polynomial is constant.

The results of numerical optimisation depend heavily on normal vector \mathbf{n} .

In the case $\mathbf{n} = (n_x, n_y, 0)$ $A = B = 0$ and the coefficients for the envelopes $A_1 = B_1 = B_2 = 0$, so this case is analogous to relative distance metric (6) (see Figures 3, 4).

In the case $\mathbf{n} = (0, 0, 1)$ the expression for Δ_2 is simplified due to $A = B = A_1 = B_1 = A_2 = B_2 = 0$, so $E_{\pm} = \frac{a^2}{2} (k^2 + 1) \pm \frac{a^2}{2} (k^2 - 1)$ and the optimisation procedure is not applicable to the problem (Figure 5).

For the general choice of the vector \mathbf{n} the envelopes are more complex asymmetric curves with several beating frequencies (Figures 6, 7), still the aforementioned technique produces the numerical optimised results (Figures 8, 9)

NELDER-MEAD OPTIMIZATION ALGORITHM

One of the popular non-gradient methods for solving unconstrained optimization problems is the Nelder-Mead simplex method (do not confuse with the simplex method for linear programming problems). The idea behind the method is first to initialize a simplex with $n + 1$ vertices in the n -dimensional phase space and then to modify the simplex with the operations of reflection, expansion, contraction, and shrinkage, depending on the objective function values at the vertices. The algorithm is simple and easily programmable. Its description can be found in the paper of Lagarias et al.¹⁴ This

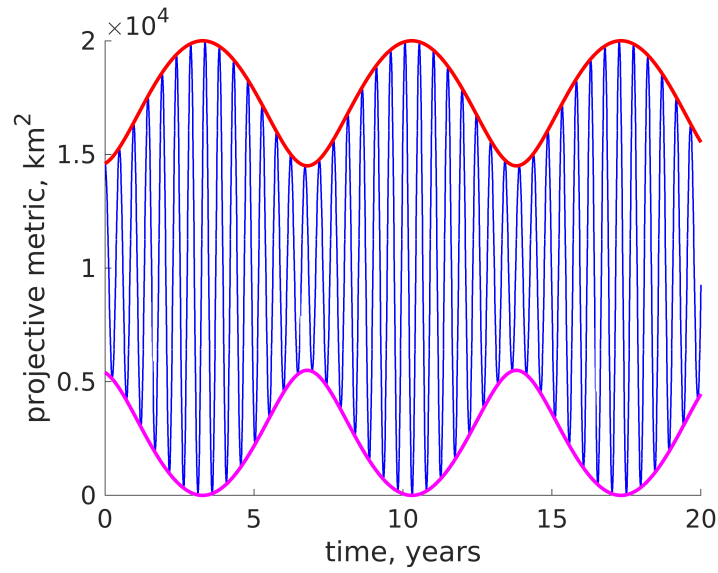


Figure 3. Projective metric behaviour without optimisation, $\mathbf{n} = (n_x, n_y, 0)$

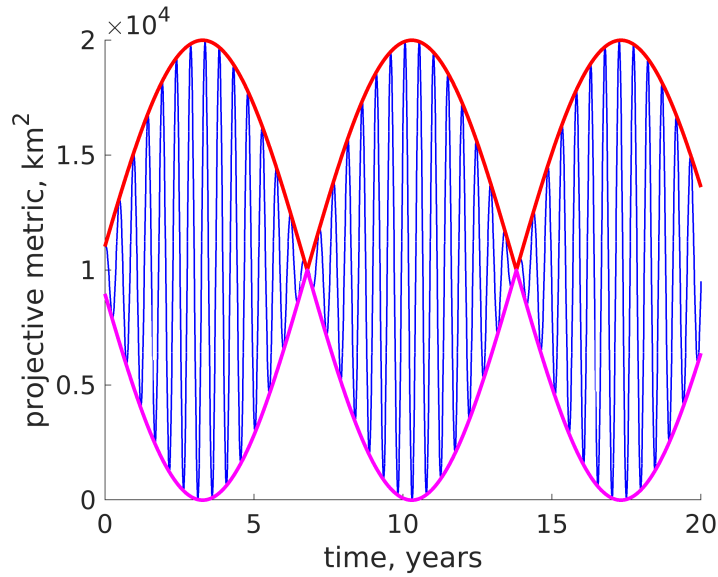


Figure 4. Projective metric behaviour after optimisation, $\mathbf{n} = (n_x, n_y, 0)$

classical algorithm is implemented in the FMINSEARCH routine, a part of the Matlab Optimization Toolbox.

In cases when the problem is initially constrained, penalty functions are added to the objective function. For example, if we want to target some value c of the relative distance so that $c(1 - \varepsilon_1) \leq \Delta r \leq c(1 + \varepsilon_2)$ at a specific time interval, the following objective function can be exploited:

$$J = (\langle \Delta r \rangle - c)^2 + k_1 \max(0, c(1 - \varepsilon_1) - m) + k_2 \max(0, M - c(1 + \varepsilon_2)) \quad (10)$$

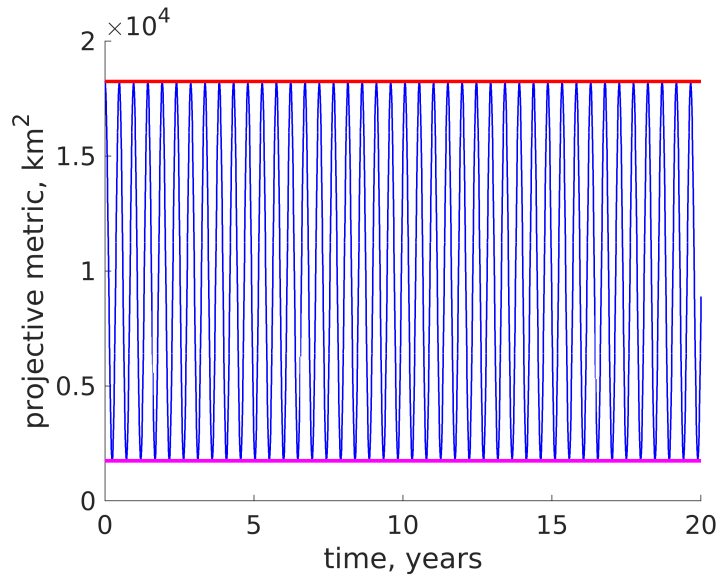


Figure 5. Projective metric behaviour with $n_z = 1$

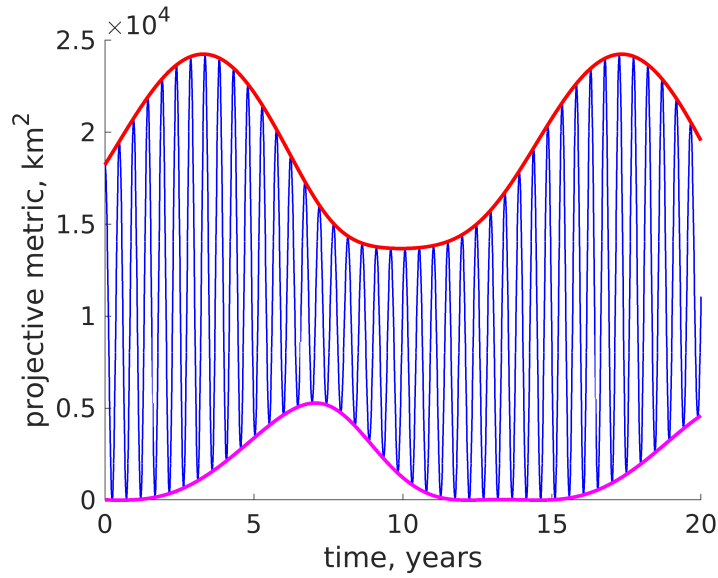


Figure 6. Projective metric behaviour with $n_x = n_y = n_z$

In this expression, $\langle \Delta r \rangle$ is the average value of $\sqrt{\Delta r^2}$ over a given time interval, $m = \min \sqrt{\Delta r^2}$, $M = \max \sqrt{\Delta r^2}$, k_1 and k_2 are some large penalty weight coefficients.

In practice, the Nelder-Mead method often performs well even for irregular, non-smooth, and noised objective functions or objective functions with dense local minima in a vicinity of one global minimum. However, when the dimension of the phase space is high, convergence to a local minimum could take much time; so, it is usually recommended to use the classical Nelder-Mead algorithm only for small-scale problems. Nonetheless, large-scale modifications of the algorithm also exist.^{15,16} These parallel versions can be effectively used in high-performance computing systems.

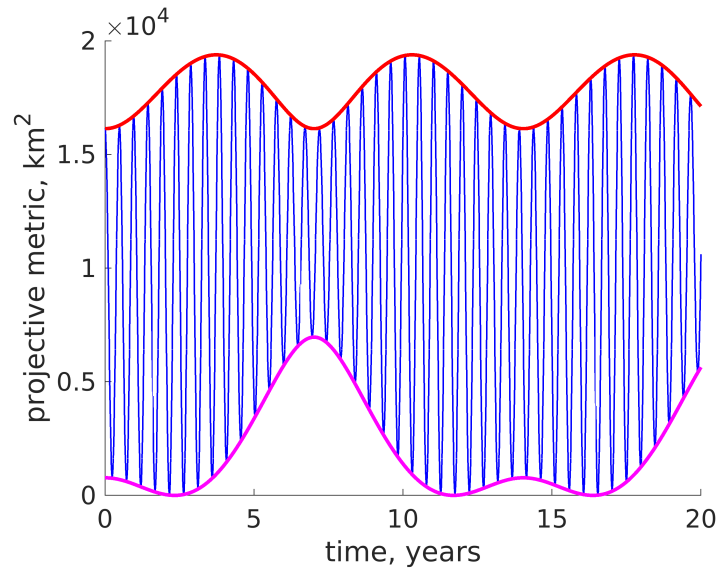


Figure 7. Projective metric behaviour with $n_x = n_z, n_y = 0$

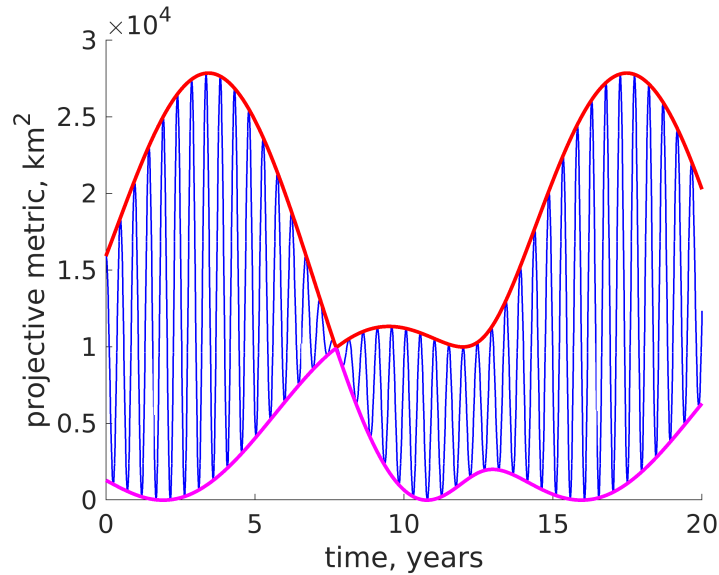


Figure 8. Projective metric behaviour with $n_x = n_y = n_z$, optimised

NUMERICAL OPTIMIZATION AND ADAPTATION TO THE EPHEMERIS MODEL

The derived analytical estimates can be exploited as an initial guess for the Nelder-Mead optimization procedure in a high-order LP approximation model. The 15th order of the LP series expansion is quite accurate for the reference Lissajous orbit selected. The termination tolerances of Matlab's FMINSEARCH routine for the objective function and the vector of optimized variables have been set to $1e - 8$.

In the relative distance-based performance metric (10) with $c = 6.6845871 \cdot 10^{-7}$ (the non-

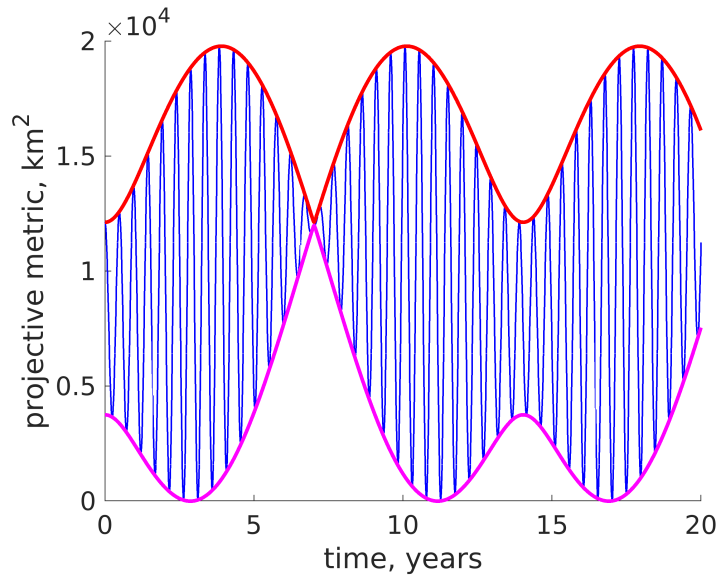


Figure 9. Projective metric behaviour with $n_x = n_z, n_y = 0$, optimised

dimensional equivalent of 100 km), the penalty weight coefficients k_1 and k_2 both equal 10^7 . The analytical estimate (9) for the time a formation naturally keeps acceptable performance is used as the length of the optimization interval.

The numerical optimization in the 15th-order approximation model is followed by the adaptation of resulting absolute spacecraft trajectories to the high-fidelity model incorporating the gravitational attraction of the Sun and all the planets up to Saturn, as well as the solar radiation pressure force (the area-to-mass-ratio of $0.01 \text{ m}^2/\text{kg}$ is assumed for all spacecraft). In all the examples below, the initial date of Jan 1, 2020 is used. It requires just 3-8 multiple-shooting iterations to converge.

The evolution of the relative distance for a two-spacecraft formation in several models of motion is compactly shown in Fig. 10. The upper and lower bounds $\varepsilon_1 = 1 - \sqrt{1 - \varepsilon}$, $\varepsilon_2 = \sqrt{1 + \varepsilon} - 1$ with $\varepsilon = 0.1$ are indicated by dashed lines. In the 15th-order approximation model, the analytical guess slightly violates the bounds, which is then successfully eliminated by the numerical optimization. The subsequent adaptation to the ephemeris model has almost no influence on the performance.

In higher orders of approximation, the difference between the planar and vertical frequencies is known to be less than in the linear approximation. Thus, the conservative estimate (9) can usually be refined by substituting $\omega_2 - \omega_1$ in the denominator instead of $\delta = \omega_p - \omega_v$. The analytical guess sometimes appears excellent even for longer intervals. For example, it is managed to optimize the half-year formation design of Fig. 10 over the one-year interval (Fig. 11). In some cases, however, it is necessary to relax the ε tolerance when proceeding to the numerical optimization. For sophisticated performance metrics, natural constraints on ε can exist in high-fidelity models.

CONCLUSION

The proposed semianalytical technique based on the powerful tool of Lindstedt-Poincaré series has appeared to be an effective approach to the rather complicated problem of designing libration point formations with various performance metrics. The series of any order are readily param-

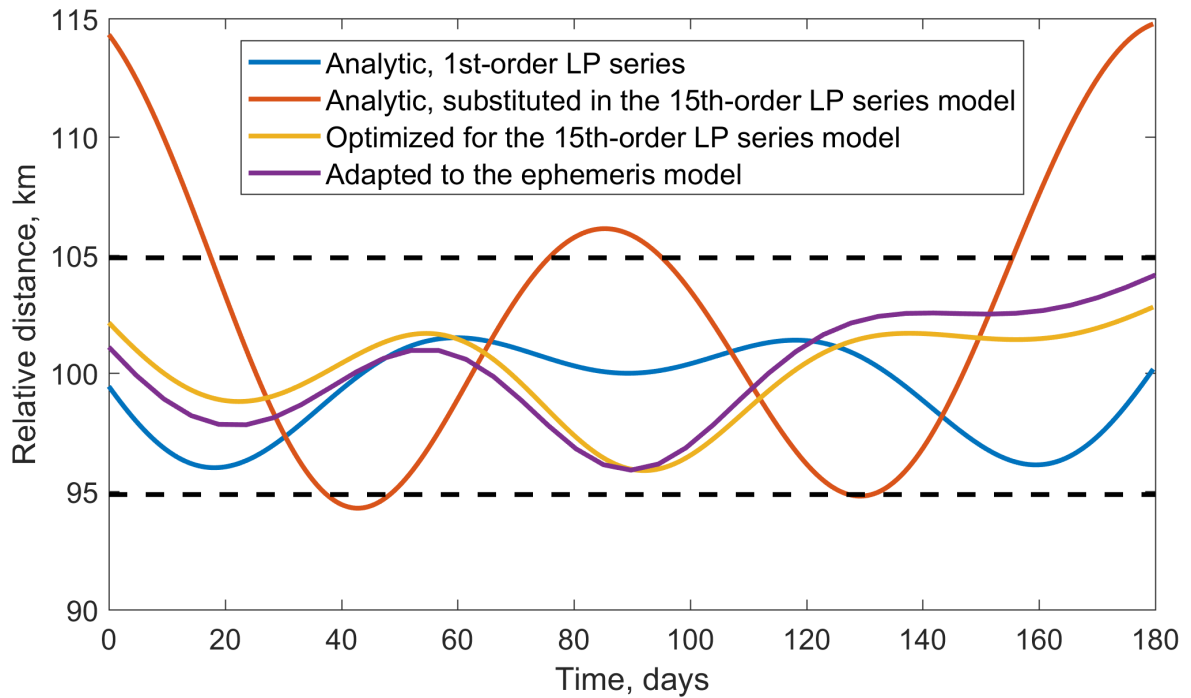


Figure 10. Relative distance behavior for a two-spacecraft formation in different models of motion

eterised by just four design parameters, which opens the road to such non-gradient optimisation techniques as the classical Nelder-Mead simplex algorithm. Numerical integration is thus totally avoided.

The analysis of low-order expressions for the performance metric makes it often possible to obtain an initial guess for the numerical optimisation procedure. This drastically speeds up the convergence or is even its prerequisite.

The explicit analytical derivations have been presented for the relative distance-based performance metric and projective performance metric in the case of two-spacecraft formation. The optimal design is found so that the relative distance variations for half a year are no greater than 5-6% in the 15th-order approximation model and the ephemeris model. The same stability level proved to be achievable for the one-year ballistic flight.

ACKNOWLEDGMENTS

The research was supported by the Russian Science Foundation (RSF) grant 19-11-00256.

REFERENCES

- [1] Gurfil, P. and Casdin, N.J., Dynamics and Control of Spacecraft Formation Flying in Three-Body Trajectories, *AIAA Guidance, Navigation, and Control Conference and Exhibit*, Montreal, Canada, August 6–9, 2001, Paper AIAA 2001-4026, 11 p.
- [2] Hamilton, N.H., Folta, D., and Carpenter, R., Formation Flying Satellite Control Around the L2 Sun-Earth Libration Point, *AIAA/AAS Astrodynamics Specialist Conference and Exhibit*, Monterey, CA, USA, August 5–8, 2002, Paper AIAA 2002-4528, 11 p.

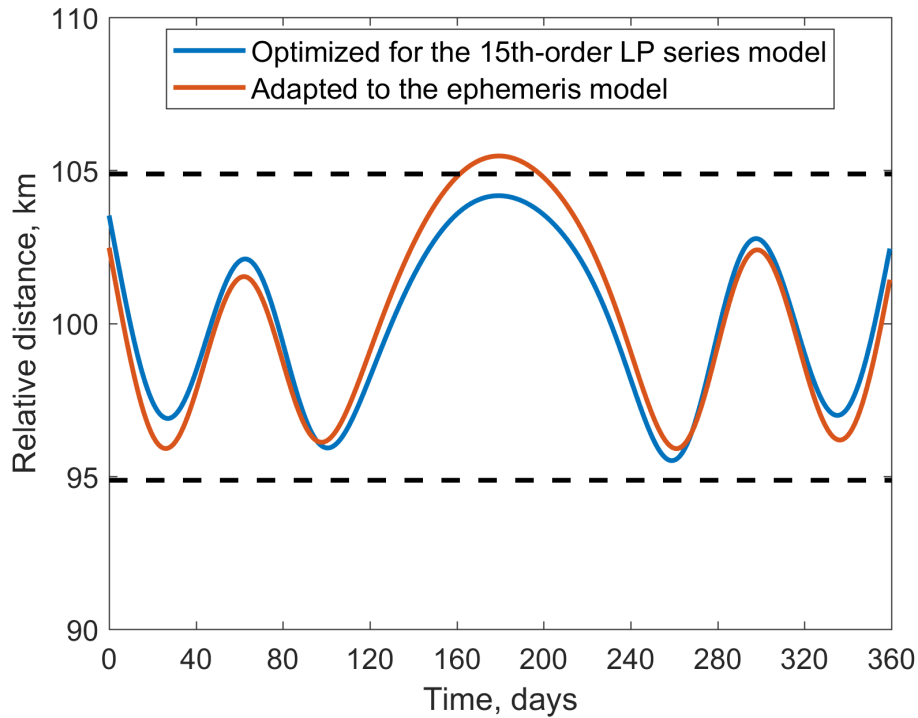


Figure 11. Relative distance behavior for a two-spacecraft formation optimized over the extended time interval

- [3] Scheeres, D.J., Hsiao, F.Y., and Vinh, N.X., Stabilizing Motion Relative to an Unstable Orbit: Applications to Spacecraft Formation Flight, *Journal of Guidance, Control, and Dynamics*, Vol. 26, No. 1, 2003, pp. 62–73.
- [4] Hsiao F. Y., Scheeres D. J. Design of spacecraft formation orbits relative to a stabilized trajectory *Journal of Guidance, Control, and Dynamics*, 2005, Vol. 28 (4), pp. 782-794.
- [5] Marchand, B.G. and Howell, K.C., Control Strategies for Formation Flight in the Vicinity of the Libration Points, *Journal of Guidance, Control, and Dynamics*, Vol. 28, No. 6, 2005, pp. 1210–1219.
- [6] Serpelloni, E., Maggiore, M., and Damaren, C.J., Control of Spacecraft Formations Around the Libration Points Using Electric Motors with One Bit of Resolution, *Journal of the Astronautical Sciences*, Vol. 61, Issue 4, 2014, pp. 367–390.
- [7] Infeld, S.I., Josselyn, S.B., Murray, W., and Ross, I.M., Design and Control of Libration Point Spacecraft Formations, *Journal of Guidance, Control, and Dynamics*, Vol. 30, No. 4, 2007, pp. 899–909.
- [8] Howell, K.C. and Marchand, B.G., Natural and Non-Natural Spacecraft Formations Near the L1 and L2 Libration Points in the Sun-Earth/Moon Ephemeris System, *Dynamical Systems: an International Journal, Special Issue on Mechanics and Space Mission Design*, Vol. 20, Issue 1, 2005, pp. 149–173.
- [9] Gómez, G., Marcote, M., Masdemont, J., and Mondelo, J., Zero Relative Radial Acceleration Cones and Controlled Motions Suitable for Formation Flying, *Journal of the Astronautical Sciences*, Vol. 53, No. 4, 2005, pp. 413–431.
- [10] Héritier, A. and Howell, K.C., Regions Near the Libration Points Suitable to Maintain Multiple Spacecraft, *AIAA/AAS Astrodynamics Specialist Conference*, Minneapolis, MN, USA, August 13–16, 2012, Paper AIAA 2012-4666, 20 p.
- [11] Ferrari, F. and Lavagna, M., Suitable Configurations for Triangular Formation Flying About Collinear Libration Points Under the Circular and Elliptic Restricted Three-Body Problems, *Acta Astronautica*, Vol. 147, 2018, pp. 374–382.
- [12] Gómez, G., Jorba, À., Masdemont, J., and Simó, C., *Dynamics and Mission Design Near Libration Point Orbits – Volume III: Advanced Methods for Collinear Points*, Vol. 4, World Scientific, 2001, pp. 36–39.
- [13] Simo, C., et al. *On the optimal station keeping control of halo orbits*, *Acta Astronautica* Vol. 15, No. 6-7 1987, pp. 391–397.

- [14] Lagarias, J. C., Reeds, J. A., Wright, M. H., Wright, P. E. (1998). *Convergence properties of the Nelder–Mead simplex method in low dimensions*. SIAM Journal on optimization, 9(1), pp.112–147.
- [15] Lee, D., Wiswall, M. *A parallel implementation of the simplex function minimization routine*. Computational Economics, Vol. 30, No.2, 2007, pp. 171–187
- [16] Klein, Kyle, and Julian Neira. *Nelder-mead simplex optimization routine for large-scale problems: A distributed memory implementation.*, Computational Economics, Vol. 43, No. 4, 2014 pp. 447–461.

APPENDIX

Transformation Between Relative and Differential Parameters of Linearized Relative Motion

The orbit of the first spacecraft is described by the expressions

$$\begin{aligned}x_1 &= \alpha \cos(\omega_p t + \phi_1) \\y_1 &= -\kappa \alpha \sin(\omega_p t + \phi_1) \\z_1 &= \beta \cos(\omega_v t + \phi_2),\end{aligned}$$

For the orbit of the second spacecraft, we have

$$\begin{aligned}x_2 &= (\alpha + \Delta\alpha) \cos(\omega_p t + \phi_1 + \Delta\phi_1) \\y_2 &= -\kappa(\alpha + \Delta\alpha) \sin(\omega_p t + \phi_1 + \Delta\phi_1) \\z_2 &= (\beta + \Delta\beta) \cos(\omega_v t + \phi_2 + \Delta\phi_2)\end{aligned}$$

Since the relative position vector $\Delta\mathbf{r}$ satisfies the same linear equations, its components can be written as follows:

$$\begin{aligned}\Delta x &= A_x \cos(\omega_p t + \theta_1) \\ \Delta y &= -\kappa A_x \sin(\omega_p t + \theta_1) \\ \Delta z &= A_z \cos(\omega_v t + \theta_2)\end{aligned}$$

The relation between $A_x, A_z, \theta_1, \theta_2$ and $\Delta\alpha, \Delta\beta, \Delta\phi_1, \Delta\phi_2$ can be easily derived from the equations $\Delta x = x_2 - x_1, \Delta y = y_2 - y_1, \Delta z = z_2 - z_1$. The solution is given by the following relationships:

$$\begin{aligned}\Delta\phi_1 &= \arctan(A_x \sin(\theta_1 - \phi_1), A_x \cos(\theta_1 - \phi_1) + \alpha) \\ \Delta\phi_2 &= \arctan(A_z \sin(\theta_2 - \phi_2), A_z \cos(\theta_2 - \phi_2) + \beta) \\ \Delta\alpha &= -\alpha + \alpha \cos \Delta\phi_1 + A_x \cos(\theta_1 - \phi_1 - \Delta\phi_1) \\ \Delta\beta &= -\beta + \beta \cos \Delta\phi_2 + A_z \cos(\theta_2 - \phi_2 - \Delta\phi_2)\end{aligned}$$

The coefficients for the envelope in the projected relative metric

For the square of amplitude

$$F_1^2 + F_2^2 = A_0 + A_1 \cos q + B_1 \sin q + A_2 \cos 2q + B_2 \sin 2q.$$

$$\begin{aligned}
A_0 &= \frac{A_x^4 \kappa^4}{4} (1 - n_y^2)^2 + \frac{A_x^4 \kappa^2}{2} (n_x^2 n_y^2 - n_z^2) + \frac{A_x^4}{4} (1 - n_x^2)^2 + \frac{A_z^4}{4} (1 - n_z^2)^2 \\
&\quad + A_x^2 A_z^2 n_z^2 (\kappa^2 n_y^2 + n_x^2) \\
A_1 &= A_x^3 A_z n_x n_z (\kappa^2 n_y^2 + \kappa^2 + n_x^2 - 1) - A_x A_z^3 n_x n_z (n_x^2 + n_y^2) \\
A_2 &= \frac{A_x^2 A_z^2}{2} (n_x^2 n_z^2 + n_y^2 - \kappa^2 n_y^2 n_z^2 - \kappa^2 n_x^2) \\
B_1 &= A_x^3 A_z \kappa n_y n_z (\kappa^2 n_y^2 - \kappa^2 + n_x^2 + 1) - A_x A_z^3 \kappa n_y n_z (n_x^2 + n_y^2) \\
B_2 &= -A_x^2 A_z^2 \kappa n_x n_y n_z^2 (n_x^2 + n_y^2)
\end{aligned}$$